

Tomasz CHMIELEWSKI*

Paweł NOWAK**

IMPEDANCE CHARACTERISTICS OF PYRITES IN RELATION TO THEIR COLLECTORLESS FLOTATION

The microflotation test, rest potential and interfacial impedance measurements have been performed for various pyrites to correlate flotation of pyrites with their electrochemical properties. It was shown that pyrites exhibiting a low corrosion current floated very well in relation to pyrites of higher corrosion currents. On the basis of performed electrochemical measurements, mechanism of pyrite corrosion in aqueous environment was proposed.

INTRODUCTION

The main feature of electrochemical methods, which makes them so attractive in the investigations of the surface properties of the conducting materials, is the possibility to perform the *in situ* experiments. The impedance spectroscopy (Macdonald, 1987) has become the most widely used electrochemical technique. The principal advantage of the impedance spectroscopy is the feasibility of determining both the kinetics of the electrochemical processes taking place at the electrode surface and the structure of the electrical double layer. The electrochemical investigations of pyrite have been carried out for a long time (Mayer, 1979, Hamilton and Woods, 1981, Ennaoui et al., 1986, Pang et al., 1990, Ahlberg et al., 1990, Ramprakash et al., 1991). Particularly, during the last few years there have appeared many papers concerning the surface properties of pyrite and most of authors applied the electrochemical methods. Such an interest in surface chemistry of pyrite results from a growing requirement of the environmental protection and is associated with the need of removal of pyrite, mainly from coal. Since even a short review on the electrochemical works would require a vast space, only general comments will be made here.

During an interaction of pyrite with an oxidative aqueous solution, decomposition of pyrite takes place leading to two surface products: sulfide oxidation products containing sulfur enriched sulfide and/or elemental sulfur and iron oxidation products (oxides, hydroxides, carbonates and sulfoxylates of iron). The former are thought to promote the hydrophobicity of pyrite surface while the later are believed to make the surface hydrophilic.

Among numerous electrochemical works concerning pyrite, only in few (Pang et al., 1990,

* Institute of Inorganic Chemistry and Metallurgy of Rare Elements, Technical University of Wrocław, Wybrzeże Wyspiańskiego 27, 50-370 Wrocław, Poland

** Institute of Catalysis and Surface Chemistry, Polish Academy of Science, ul. Niezapominajek 1, 30-239 Kraków, Poland

Mikhlin and Tomashevich, 1990) the impedance spectroscopy was used. This is a consequence of difficulties in interpretation of the results of interfacial impedance measurements of mineral electrodes. In comparison to other electrochemical techniques (for example: cyclic voltammetry), the interpretation of the impedance measurements requires advanced calculations to be involved.

In this work the authors applied interfacial impedance spectroscopy (IIS) to reveal the difference in surface properties of pyrites, which cause different behavior of pyrites in flotation. The aqueous oxidation of pyrite surface was considered to be a corrosion process and the rates of pyrites surface oxidation were determined from the measured electrochemical data.

2. EXPERIMENTAL

Materials

The symbols and origin of pyrites used in experiments are specified in Table 1. Electrodes have been made from hand picked samples of different coal and mineral pyrites. Small samples of selected pyrites were also crushed and dry-screened in order to provide the suitable particle

Table 1. Characteristics of pyrites.

SYMBOL OF SAMPLE	SAMPLE ORIGIN	TYPE OF CONDUCTIVITY
MP1	mineral pyrite (Huanzala, Peru)	n
MP2	mineral pyrite (Huanzala, Peru)	n
MPE	mineral pyrite (Elba)	p
CPIA1	coal pyrite (Iowa, USA)	p
CPIA2	coal pyrite (Iowa, USA)	p
CP1U	coal pyrite (unknown origin)	p
ILL#6	coal pyrite (Illinois #6 coal, USA)	p
CP,PL1	coal pyrite (Halemba Mine, Poland)	p
MPRT	mineral pyrite (Rio Tinto, Spain)	p

size fraction for microflotation experiments.

More details regarding the construction of pyrite electrodes are given in previous works (Chmielewski and Lekki, 1989; Chmielewski and Wheelock, 1991).

Microflotation tests

Microflotation experiments were conducted in a monobubble Hallimond tube equipped with a calibrated receiver which allowed a continuous monitoring of the recovered particles during the course of a test. A sample of 0.68 g of pyrite was placed in the Hallimond tube and conditioned for 10 min. in 120 cm³ of water. Flotation was then initiated with air at a flow rate

of 37.5 cm³/min. Microflotation tests were conducted using distilled water at natural pH of 6.9 measured prior to experiments. To eliminate the mechanical carryover of pyrite particles during flotation in the Hallimond tube, relatively large particles (from the size fraction of 0.10-0.16 mm) were used.

It was established earlier (Drzymala and Lekki 1989, Drzymala et al. 1992) that the mechanical carryover in our Hallimond tube was governed by the so-called flotometric equation in the form: $D \cdot (1/\rho') = 0.022 \pm 0.002$ g/cm², where D is the maximum size of entrained particle, while ρ' is the density of the particle in water. Thus, for pyrite having density equal to 5.0 ($\rho' = 4.0$) the maximum size of particle ^{which can} able to be entrained was equal to 0.06 mm.

To reduce excessive surface oxidation the time between sample preparation and flotation test was less than 40 minutes.

Electrochemical measurements

Electrode potential was recorded with the system consisting of potentiostat, A/D transducer, and microcomputer to control the potential changes. The potential sampling frequency was 600 measurements/s and the accuracy of measurements equal to 1 mV. IIS measurements were performed in the frequency range of 65535 - 0.001 Hz using a system consisting of 1250 Solartron Frequency Response Analyzer, 1286 Solartron Electrochemical Interface and HP 310 Computer. Three electrode system was applied with the pyrite as a working electrode, saturated calomel electrode (SCE) as the reference electrode, and an iron wire electrode as a counter. The iron electrode was properly shaped to provide the uniform electric field distribution.

Impedance measurements required the system to be in a steady state. Therefore, to minimize the change of electrode properties during measurements caused by corrosion process, the solution has been deoxygenated with argon for at least 1 hour. High purity argon (containing less than 20 ppm O₂) was additionally passed over a heated copper catalyst to reduce further the oxygen concentration to below 1 ppm. The measurements were performed after 1000 seconds of conditioning the electrode in a slightly alkaline 0.1 M solution of sodium tetraborate, Na₂B₄O₇ of pH 9.2 which was close to pH used in pyrite flotation.

RESULTS AND DISCUSSION

Microflotation experiments

For pyrite samples specified in Table 1 (except for CPU1), we performed a series of microflotation tests and their results are collected in Fig. 1. It can be seen from Fig. 1 that pyrites exhibited significant differences in collectorless floatabilities and they can be divided into three categories: easy floating (CP, PL1, MP1), medium floating (MPE, MPR), and nonfloating (CPIA, III#6) pyrites. On the basis of the numerous literature data it can be said that the main reason for a poor pyrite flotation is the formation of a surface layer of hydrophilic oxidation products. To evaluate the rate of the formation of these products, in this work we applied the Interfacial Impedance Spectroscopy (IIS) measurements.

The pyrite - solution interface as a corroding system

When a semiconducting mineral undergoes the dissolution, the process may always be

considered as the corrosion process (Nowak et al., 1984). A schematic representation of the process is presented in Fig.2. For the oxidative dissolution, two independent reaction take place simultaneously at the pyrite surface: the anodic dissolution of the mineral and the cathodic reduction of the oxidant (oxygen in most cases).

For a single electrode reaction the density of the current passing through the electrode surface may be expressed, after differentiation with respect to E and rearrangement by the following equation:

$$R_p = \frac{dE}{dI} = \frac{RT}{nF} \frac{1}{(\alpha + \beta) I^o} = \frac{RT}{nF} \frac{1}{I^o} \quad (1)$$

For a simple electrode reaction $\alpha + \beta = 1$ and one may calculate exchange current density (ECD) from equation (1) without the knowledge about the mechanism of the reaction. Therefore, the ECD can be measured by cycling the electrode potential around the equilibrium potential with a small voltage amplitude and calculating the derivative dE/dI , called the Faradaic reaction resistance, R_p . Similar procedure is possible in the case of a corroding system illustrated in Fig.2. Provided that the equilibrium potentials of the two electrode reactions differ significantly from each other, one may write the following equation for the density of current flowing through the electrode surface:

$$I = I_1^o \exp \left[\frac{\alpha_1 n_1 F}{RT} (E - E_1^o) \right] - I_2^o \exp \left[\frac{-\beta_2 n_2 F}{RT} (E - E_2^o) \right] \quad (2)$$

At the corrosion potential, E_{corr} , the anodic and cathodic counterparts of the current flowing through the electrode are the same and equal to the corrosion current density (CCD) or I_{corr} . Therefore, the total current flowing through the electrode equals zero. After differentiation and rearrangement one obtains:

$$R_p = \frac{dE}{dI} = \frac{RT}{F} \frac{1}{I_{corr} (\alpha_1 n_1 + \beta_2 n_2)} \quad (3)$$

In contrary to the case of a simple electrode reaction (Eqs 1 and 2), for the corroding system illustrated in Fig.2, $n_1 \neq n_2$ and $\alpha_1 + \beta_2 \neq 1$. Thus, to calculate I_{corr} the values of α , β and n must be known from independent sources. The values of α and β are for all electrochemical reactions within the range $0.2 < \alpha < 0.8$ (with the exception of non-degenerated

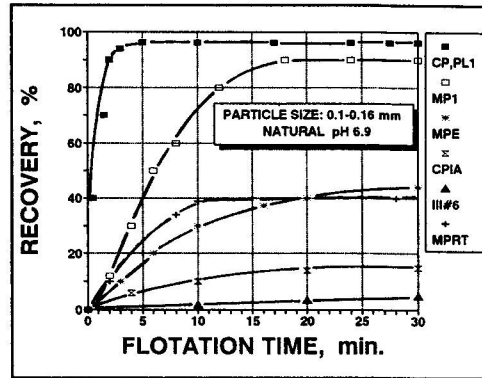


Figure 1. Results of microflotation tests for different pyrite samples.

semiconductors) and n is usually the small integer numbers. Thus, at least a reasonable estimation of the CCD is possible for any corroding system. Similarly to a simple electrode reaction, a small perturbation of the electrode potential for the corroding electrode and the calculation of the dE/dI derivative suffice to measure the CCD. The advantage of using the IIS technique over potentiodynamic methods is that, due to the small voltage amplitude, the properties of the electrode do not change during the measurements.

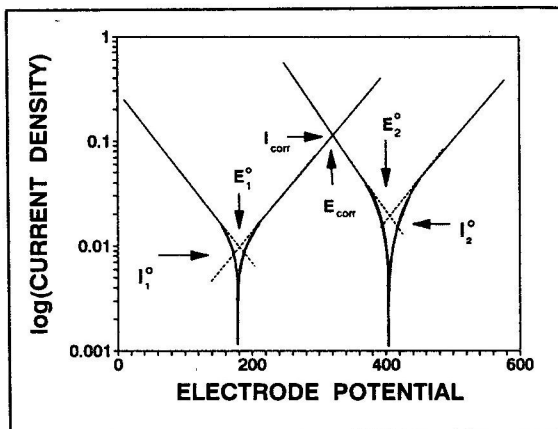


Figure 2. Potential - current density schematic relationship for a corrosion process.

The electrical equivalent circuit for a pyrite electrode

The key problem in analysis of an electrochemical system by the IIS method is assigning

a proper electrical equivalent circuit (EEC). The universal EEC for a semiconductor electrode is presented in Fig.3a. The total electrode impedance may be divided into the interfacial impedance and bulk semiconductor impedance connected in series. For the electrode made of natural pyrite, the impedance in the bulk of the solid may be neglected due to the high concentration of free charge carriers, so an EEC can be reduced to the form presented in Fig.3b. In Fig.3 CPA1 is a constant phase element representing capacitance of space charge layer in the semiconductor, CPA2 - constant phase element representing capacitance of the electrical double layer at the electrode surface, R - resistivity of the space

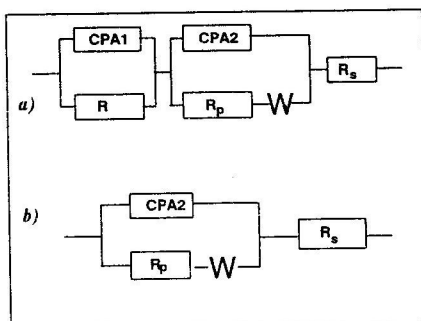


Figure 3. Electrical equivalent circuits for a semiconducting electrode.

charge layer in the semiconductor, R_p - Faradaic reaction resistivity, W - diffusional impedance, and R_s - ohmic resistance of the solution and the electrode. The EEC presented in Fig.3b is also only the approximation. A detailed analysis of the interfacial impedance of an electrode with a rough surface is given in the work of de Levie (1990). The analysis used by de Levie, however, leads to the frequency - dependent R_p value, which can be determined only with the accuracy of a multiplicative factor. Furthermore, the theory developed by de Levie is now applicable only for the most simple systems. Thus, an approximation of so called "constant phase elements" is used in this work to describe the interfacial impedance (Fig.3). The calculated R_p value is a mean value for the frequency range used and is related to the geometric area of the

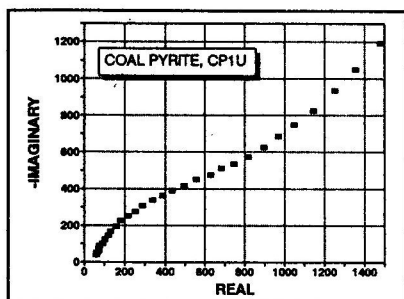


Figure 4. Interfacial impedance spectrum for pyrite electrode in 0.1 M $\text{Na}_2\text{B}_4\text{O}_7$ solution.

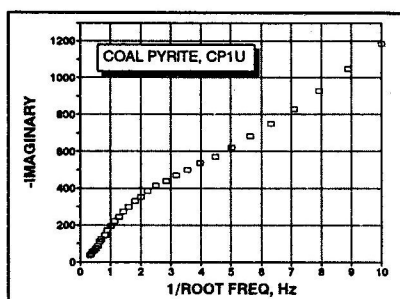


Figure 5. Imaginary versus $1/\sqrt{\omega}$ for pyrite electrode in 0.1 M $\text{Na}_2\text{B}_4\text{O}_7$ solution.

electrode. For a series of measurements carried out with different samples of the same mineral, same surface treatment, and in the same range of the frequency, the obtained results should be consistent. A typical impedance spectrum of pyrite electrode in $\text{Na}_2\text{B}_4\text{O}_7$ solution is presented in Fig.4. The plot has a shape of semicircle, whose radius is equal to R_p (Tab.2). For a sufficiently low frequency semicircle assumes the shape of a straight line. For that range of frequencies the diffusion is the limiting step of the overall electrode process, and the impedance may be expressed by the equation:

$$W = \frac{RT(j-1)}{n^2 F^2 c \sqrt{2D\omega}} \quad (4)$$

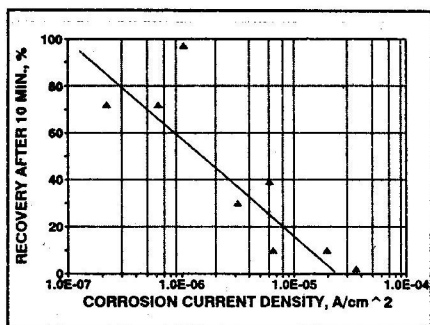


Figure 6. Flotation recovery - corrosion current density plot for pyrites.

Plotting the imaginary part of the electrode impedance versus reciprocal of the root of frequency (see Fig.5) one can calculate either the concentration of the diffusing species, if the diffusion coefficient is known, or the diffusion coefficient, if the concentration is known.

Most surprising observation from the data presented in Table 2 are big differences between R_p values determined for various samples of the same mineral. It means that different pyrite samples exhibit different susceptibility to oxidation in aqueous environment leading to a different surface coverage

by hydrophilic oxidation products within the same time of contact with the solution. Therefore, the differences in ability to oxidation is most likely the reason of floatability differences observed for pyrites in Fig.1. The relationship between the recovery of pyrite after 10 min. flotation and

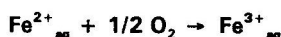
corrosion current for different pyrites is plotted in Fig.6.

For pyrites, exhibiting in IIS measurements evident diffusional limitation, we estimated (Eq.4) the concentration of diffusing species assuming the number of transferred electrons to be 1 or 2 and the diffusion coefficient $D = 10^{-5}$. These numbers are typical for simple inorganic species. The estimated values of concentration (Tab.2) exceed (several orders) the expected concentration of oxygen in the solution. Thus, it is clear that diffusing species in the system is not oxygen. The mechanism of the aqueous oxidation of pyrite most likely involves the following steps:

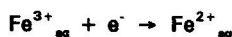
anodic reaction:



$\text{Fe}^{2+}_{\text{aq}}$ ions diffuse to the bulk of the solution and then



cathodic reaction:



The Fe^{2+} ions are oxidized by oxygen dissolved in the solution. Additional evidences confirming this mechanism were obtained from rest potential-time measurements shown in Figs. 7 and 8. The MP1 pyrite exhibiting very low corrosion current (Tab.2) has rather constant rest potential

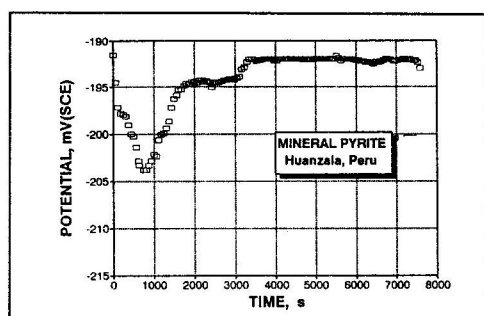


Figure 7. Rest potential - time plot for MP1 pyrite electrode in 0.1 M tetraborate solution.

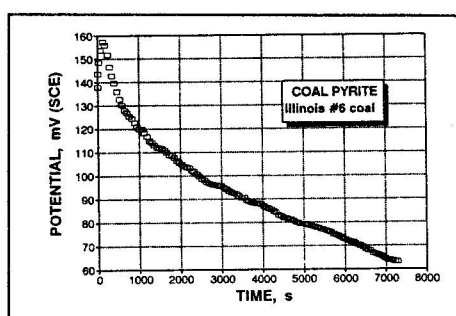


Figure 8. Rest potential-time plot for Ill#6 pyrite electrode in 0.1M tetraborate solution.

(Fig.7) due to slow changes of both the electrode surface properties and concentrations of all species at the electrode surface. For pyrite Ill#6, showing higher corrosion current (Tab.2), the continuous decrease of the rest potential was observed for a long time (Fig.8), apparently due to the accumulation of Fe^{2+} ions at the electrode surface.

For pyrites exhibiting very low corrosion current (Table 2), the oxidation is slow and such iron compounds as hydroxides, carbonates and others have enough time to dissolve and diffuse away to the bulk of the solution. Thus, the surface of pyrites enriches in sulphur or sulphur excess pyrite. This leads to an increase in their flotation.

When pyrites exhibit a high corrosion current, the formation of the hydrophilic iron compounds on the mineral surface is very fast and these products diffuse away from the surface

Table 2. Results of IIS measurements for pyrite electrodes.

PYRITE ELECTRODE	REST POTENTIAL, mV (SCE)	POLARIZATION RESISTANCE $\Omega \cdot \text{cm}^2$	CORROSION CURRENT A/cm^2	ESTIMATED CONCENTRATION, mola/l	
				$c_{\text{est}}, n=2$	$c_{\text{est}}, n=1$
MP1	- 169	$1.46 \cdot 10^5$	$2.63 \cdot 10^{-7}$	-	-
	- 194	$1.68 \cdot 10^5$	$2.29 \cdot 10^{-7}$		
	- 205	$1.67 \cdot 10^5$	$2.30 \cdot 10^{-7}$		
	- 162	$1.74 \cdot 10^5$	$2.21 \cdot 10^{-7}$		
	- 195	$2.30 \cdot 10^5$	$1.67 \cdot 10^{-7}$		
MP2	- 168	$4.54 \cdot 10^4$	$8.45 \cdot 10^{-7}$	-	-
	- 176	$9.18 \cdot 10^4$	$4.18 \cdot 10^{-7}$		
	- 176	$6.37 \cdot 10^4$	$6.03 \cdot 10^{-8}$		
CPIA1	+ 137	$1.54 \cdot 10^3$	$2.49 \cdot 10^{-5}$	$3.3 \cdot 10^{-5}$	$13.2 \cdot 10^{-5}$
	+ 86	$1.75 \cdot 10^3$	$2.19 \cdot 10^{-5}$		
	0	$3.22 \cdot 10^3$	$1.19 \cdot 10^{-5}$		
CPIA2	+ 21	$4.93 \cdot 10^3$	$7.79 \cdot 10^{-6}$	-	-
	- 56	$6.58 \cdot 10^3$	$5.84 \cdot 10^{-6}$		
	- 102	$6.63 \cdot 10^3$	$5.79 \cdot 10^{-6}$		
CP1U	+ 69	$5.43 \cdot 10^2$	$5.42 \cdot 10^{-5}$	$3.2 \cdot 10^{-5}$	$12.8 \cdot 10^{-5}$
	+ 126	$6.58 \cdot 10^2$	$5.84 \cdot 10^{-5}$		
	+ 100	$7.54 \cdot 10^2$	$5.09 \cdot 10^{-5}$		
MPE	- 165	$1.22 \cdot 10^4$	$3.15 \cdot 10^{-8}$	$2.9 \cdot 10^{-5}$	$11.6 \cdot 10^{-5}$
CP,PL1	- 205	$3.66 \cdot 10^4$	$1.05 \cdot 10^{-8}$	-	-
MPRT	- 433	$6.34 \cdot 10^3$	$6.06 \cdot 10^{-8}$		
ILL#6	+ 81	$1.04 \cdot 10^3$	$3.69 \cdot 10^{-5}$	$1.06 \cdot 10^{-4}$	$4.24 \cdot 10^{-5}$
	+ 187	$9.75 \cdot 10^2$	$3.94 \cdot 10^{-5}$		
	+ 170	$1.21 \cdot 10^3$	$3.17 \cdot 10^{-5}$		

only partially. As a result, the hydrophilic iron oxidation species predominate on the pyrite surface and cause a decrease in pyrite flotation.

Since the rate of transport in the solution does not depend on the solid properties, the flotation behavior of pyrite can be easily predicted from the measured R_p values.

Acknowledgement: The financial support of the Polish Committee for Scientific Research (Grant No.3 0336 91 01) is gratefully acknowledged.

REFERENCES

Ahlberg, E., Forssberg, K.S.E., and Wang, X., 1990. The surface oxidation of pyrite in alkaline solutions., *J. Appl. Electrochem.* 20:1033-1039.

Chmielewski T. and Lekki J., 1989, Electrochemical investigation on adsorption of potassium ethyl xanthate on galena, *Miner. Engng.*, 2(3):387-391.

Chmielewski T. and T.D.Wheelock, 1991, Thioglycolic acid as a flotation depressant for pyrite., *Flotation and Utilization of High Sulfur Coals IV*, P.R.Dugan, D.R.Quigley, and Y.A.Attia (Editors), Elsevier, Amsterdam, pp. 295-307.

Drzymała J. and Lekki J., 1989, Flotometry - another way of characterizing flotation, *J.Colloid Interface Sci.*, 130(1), 205-210.

Drzymała J., Chmielewski T., Wheelock T.D., Birlingmair D., and Wolters K.L., 1992, Flotometry based on the modified Hallimond tube., *Inst.Min.Met., Sec.C (in press)*.

Ennaoui, A., Fichter, S., Jaegermann, W., and Tributsch, H., 1986. Photochemistry of highly quantum efficient single-crystalline n-FeS₂. *J. Electrochem. Soc.*, 133:97-106.

Hamilton, I.C. and Woods, R., 1981. An investigation of surface oxidation of pyrite and pyrrhotite by linear potential sweep voltammetry. *J. Electroanal. Chem.*, 118:327-343.

de Levie, R., 1990. Fractals and rough electrodes. *J. Electroanal. Chem.*, 281:1-21.

Macdonald, J.R., 1987. Impedance spectroscopy. *J. Wiley & Sons*

Mayer, R.E., 1979. Electrochemistry of FeS₂. *J. Electroanal. Chem.*, 101:59-71.

Nowak, P., Krauss, E., and Pomianowski A., 1984. The electrochemical characteristics of the galvanic corrosion of sulfide minerals in short - circuited model galvanic cells., *Hydrometallurgy*, 12:95-110.

Pang, J., Briceno, A., and Chander S., 1990. A study of pyrite/solution interface by impedance spectroscopy. *J. Electrochem. Soc.*, 137:3447-3455.

Ramprakash, Y., Koch, D.F.A., and Woods R., 1991. The interaction of iron species with pyrite surfaces. *J. Appl. Electrochem.*, 21:531-536.

CHMIELEWSKI T, NOWAK P, 1992, Charakterystyki impedancyjne pirytów w odniesieniu do ich flotacji bezkolektorowej., *Fizykochemiczne Problemy Mineralurgii*, 25, 59 - 67

Wykonano testy mikroflotacyjne, pomiary potencjałów spoczynkowych i pomiary impedancji międzyfazowej dla różnych pirytów w celu skorelowania obserwowanych różnic we flotowalności z własnościami elektrochemicznymi minerałów. Wykazano, że piryty o niskich prądach korozji flotowały bardzo dobrze w przeciwieństwie do słabej flotacji pirytów o wysokich prądach korozji. Na podstawie wykonanych badań elektrochemicznych zaproponowano mechanizm korozji pirytu w środowisku wodnym.